PtRu Alloy and PtRu−WO_3 Nanocomposite Electrodes for Methanol Electrooxidation Fabricated by a Sputtering Deposition Method

Kyung-Won Park,[†] Jong-Ho Choi,[‡] Kwang-Soon Ahn,[‡] and Yung-Eun Sung*[,†]

School of Chemical Engineering & Research Center for Energy Conversion & Storage, Seoul National University, Seoul 151-744, S. Korea, and Department of Materials Science & Engineering, Gwangju Institute of Science & Engineering, Gwangju 500-712, S. Korea

Received: November 12, 2003

PtRu alloy and PtRu−WO_3 nanocomposite thin-film electrodes for methanol electrooxidation were fabricated by means of a sputtering method. The structural and electrochemical properties of well-defined PtRu alloy thin-film electrodes were characterized using X-ray diffraction (XRD), Rutherford backscattering spectroscopy (RBS), X-ray photoelectron spectroscopy (XPS), transmission electron microscopy, and electrochemical measurements. The alloy thin-film electrodes were classified as follows: Pt-based (10−40 atom % of Ru) and Ru-based (60 atom % of Ru) alloy structure. Among the electrodes formed by the sputtering method, PtRu-80, with 62 atom % Pt confirmed by XRD, showed the best catalytic activity for methanol electrooxidation. In particular, surface enrichment of Pt in the PtRu alloy thin-film electrodes, e.g. 65 atom % Pt for PtRu-80, was observed by XPS. Then, based on structural and electrochemical understanding of the PtRu alloy electrodes, PtRu−WO_3 nanocomposite thin-film electrodes were formed. The well-controlled physical and (electro)chemical properties of PtRu−WO_3 showed a specific current of 22 A/g at 0.45 V vs NHE, compared to that of 12 A/g for the case of conventional PtRu alloy nanosized catalyst. The homogeneous dispersion of alloy catalyst and the well-formed nanophase structure in the PtRu−WO_3 would lead to an excellent catalytic electrode. In addition, the enhanced catalytic activity in the nanocomposite electrode was found to be closely related to proton transfer in tungsten oxide using in-situ electrochemical transmittance measurement.

Introduction

The catalytic, physical, (electro)chemical, electronic, and optical properties of nanostructure materials are extremely different from those of bulk materials.[1−3] Because the size and structure of nanoparticles have a significant effect on catalytic reactions, well-controlled nanostructures are essential for achieving efficient catalysts and in the preparation of catalysts for use in fuel cells. In particular, direct methanol fuel cells (DMFCs) have attracted considerable interest because of a variety of merits, such as low operating temperatures, ease of handling a liquid fuel, the high energy density of methanol, and applications to microsized fuel cells.[4−10] The excellent catalytic activity of platinum for methanol oxidation, especially at low temperatures, makes this metal electrocatalyst ideal for use as an anode in DMFCs. However, since pure platinum is readily poisoned by intermediates produced during methanol electrooxidation, at low temperatures, Pt-based alloy or nanocomposite catalysts alloying or mixing platinum with second or third elements need to be designed and synthesized. In general, the CO-poisoned platinum can be regenerated via the reaction of surface CO with oxygen species associated with an element such as ruthenium to yield CO_2.[11−27] Accordingly, PtRu alloy structure is extremely essential for enhanced methanol electooxidation. In addition, many efforts have been reported to modulate the composition and structure of PtRu alloy nanoparticles and investigate methanol electrooxidation in nanoparticles.

Recently, small-scale electronic devices ranging from small digital devices to microelectromechanical systems (MEMS) have attracted considerable interest. Such devices can be fabricated on a small scale, that is, they must have a small mass and volume. Accordingly, the power source for these applications should be small-sized for on-chip or integration as well as have sufficiently available capability to operate the intended devices. More recently, the miniaturization[28−30] of DMFCs, which uses methanol directly as a fuel source, has been the subject of intense study. The excellent catalytic activity of electrodes for small-sized fuel cells is strongly dependent on the thin-film electrode structure such as a nanocomposite consisting of alloy nanophases in a porous material. We recently reported on a nanocomposite structure consisting of Pt nanophase and oxide matrix that provides enhanced catalytic activity.[31,32] However, the use of conventional physical deposition methods for preparing two-phase electrodes containing nanometallic phases as catalysts and porous oxide to achieve effective catalysis and high-performance electrodes in a fuel cell is difficult. Accordingly, a sputtering system comprised of a multigun, i.e. individual guns for metal and oxide targets for alloy formation and nanocomposite structure, would be ideal.

In this paper, PtRu alloy and PtRu−WO_3 nanocomposite thin-film electrodes for enhanced methanol electrooxidation were fabricated by means of a sputtering method using multiple sputtering guns. The structural and electrochemical properties of PtRu alloy thin-film electrodes were characterized using X-ray diffraction (XRD), Rutherford backscattering spectroscopy (RBS), X-ray photoelectron spectroscopy (XPS), and electrochemical measurements. In addition, based on our structural and

* To whom correspondence should be addressed. E-mail: ysung@snu.ac.kr.
[†] Seoul National University.
[‡] Gwangju Institute of Science & Engineering.

10.1021/jp037458i CCC: $27.50
Published on Web 04/21/2004

electrochemical understanding of the PtRu alloy thin-film electrodes, the well-controlled PtRu−WO_3 nanocomposite electrode was characterized using in-situ electrochemical transmittance measurement.

Experimental Section

The PtRu alloy and nanocomposite electrode was grown using an RF magnetron sputtering system. Indium tin oxides (ITO, Samsung Corning Co, Ltd) coated on transparent glasses were used as the substrate, and Pt, Ru, and WO_3 were used as the target materials. To fabricate the PtRu alloy thin-film electrode, Pt and Ru sputtering guns were used. On the other hand, Pt, Ru, and WO_3 sputtering guns were used to produce a PtRu−WO_3 nanocomposite structure. Sputtering was carried out under an atmosphere of inert Ar gas at 40 sccm at room temperature (rt). Cu grids were also used as substrates for analysis by TEM.

XRD (Rigaku X-ray diffractometer equipped with a Cu Kα source at 40 kV and 40 mA) analyses of as-prepared electrodes were used to analyze the alloy structure. RBS was used to determine the composition of the alloy thin-film electrodes. A dose of 10 μC of He^{2+} ions was used to obtain the RBS spectra. The ions had an incident energy of 2.24 MeV and a scattering angle of 165°. Hypra (Charles Evans & Associates' simulation software program) was used for analysis of the RBS data. To analyze and compare the surface chemical states of the samples, XPS was carried out using a VG Scientific (ESCALAB 250) photoelectron spectrometer. The X-ray source was Al Kα with 1486.6 eV operating at 150 kV and 150 W. The base pressure of the system was 2×10^{-9} Torr. The TEM investigation was carried out using a Phillips CM20T/STEM electron microscope at an accelerating voltage of 200 kV.

To compare the electrochemical characteristics and performance of the electrodes with respect to methanol electrooxidation, current−potential curves were examined using a conventional three-electrode electrochemical system consisting of a deposited thin-film electrode, Pt gauze, and Ag/AgCl as the working, counter, and reference electrode, respectively at 25 °C. All potentials are reported with respect to normal hydrogen electrode (NHE). The solution of 0.5 M H_2SO_4 and 2.0 M CH_3OH in 0.5 M H_2SO_4 was stirred constantly and purged with nitrogen gas. All chemicals used were of analytical grade.

The in situ electrochemical transmittance measurement for the direct observation of a hydrogen transfer phenomena using electrochromism was an electrochemical cell for methanol electrooxidation and an optical part consisting of a He−Ne laser (633 nm) as the light source with a power meter for the detection of optical signal modulation. During the electrochemical reaction with respect to the potential, the laser was transmitted through the thin film electrode and the modulation of signal intensity was continually detected for 30 s at intervals of 0.5 s. The electrochemical cell was comprised of Pt and Ag/AgCl as the counter and reference electrodes, respectively. All potentials were reported versus a NHE. The PtRu−WO_3 nanocomposite thin-film electrode was used as the working electrode in the electrochemical cell.

Results and Discussion

PtRu Alloy Thin-Film Electrodes. The PtRu alloy thin-film electrodes were fabricated by appropriate control of the power of the sputtering guns in a sputtering deposition system.[21] PtRu-20 through -100 denote the increased power ratio of the sputtering gun of the Ru target to that of the Pt target. As the power ratio of sputtering guns increases, a Pt-based electrode would be expected to be transformed into a Ru-based alloy electrode. As shown in Figure 1, the PtRu alloy thin-film electrode shows a higher angle shift compared to the (111) peak position of pure Pt. Assuming alloy formation between Pt and Ru based on a substitutional solid solution, such a shift in Figure 1 is due to the difference in atomic size between Pt and Ru atoms. As shown in Table 1, as the amount of Ru in the alloy thin-film increases, despacing of (111) occurs and the lattice parameter in the XRD peak decreases. From the lattice parameter obtained by XRD peak position and the assumption that PtRu electrodes fabricated by sputtering method are Pt-based structures, Table 1 shows that the composition of Pt and Ru can be modulated from ca. 85 to 40 atom % Pt in PtRu alloy electrodes.[33] It has been reported that Pt can be alloyed with up to 60 atom % of Ru to form a Pt-based faced-centered cubic (fcc) crystalline structure.[34] In addition, Figure 2 shows the RBS spectra of PtRu alloy thin-film electrodes with modulated compositions of Pt and Ru. To analyze the RBS data, Hypra, a Charles Evans & Associates' simulation software program, was used (open circle, experimental data; solid line, fit data). The alloy electrodes are varied from Pt-rich to Ru-rich structures. The amount of Pt in the electrodes decreases from ~85 to 40 atom % Pt while that of Ru increases from ~15 to 60 atom % Ru, similar to results by XRD analysis. This indicates that both elemental Pt and Ru are included in the thin-film layers and involve PtRu alloy structure formation. More intensive structural analyses are currently underway.

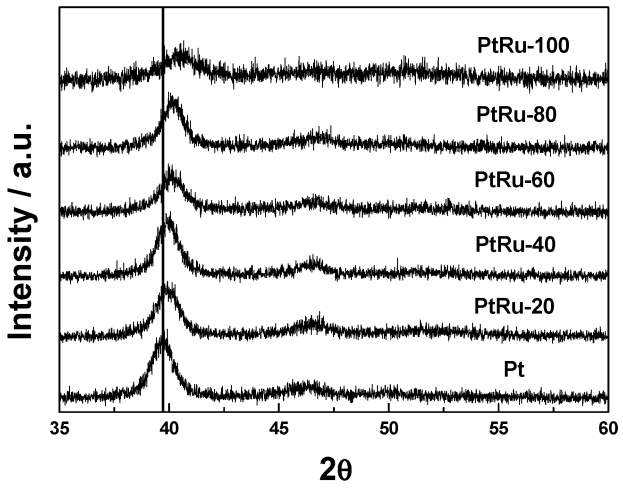

Figure 1. XRD patterns of PtRu alloy thin-film electrodes fabricated by the sputtering method. The ratio of Pt to Ru in the electrodes is easily modulated by adjusting the power of the gun used in the sputtering system.

TABLE 1: Percentage of Pt (atom % Pt) in PtRu Alloy Thin-Film Electrodes, As Determined by XRD Analysis

PtRu	d_{111} (Å)	a (Å)	atom % Pt
Pt	2.266	3.925	100.0
PtRu-20	2.256	3.907	84.6
PtRu-40	2.249	3.897	76.6
PtRu-60	2.245	3.888	69.4
PtRu-80	2.239	3.879	62.2
PtRu-100	2.223	3.851	39.8

Figure 3 shows XPS spectra of Pt4f and Ru3d in PtRu alloy thin-film electrodes deposited using the sputtering system. In the XPS spectra, the $Pt4f_{7/2}$ and $Ru3d_{5/2}$ lines of the PtRu alloy thin-film electrodes appear at ~71 and ~ 280 eV, respectively, without any peak shift, compared to the references of $Pt4f_{7/2}$ and $Ru3d_{5/2}$. However, Goodenough et al.[35] reported a lower binding energy shift in the Pt4f peak of PtRu alloy catalysts by

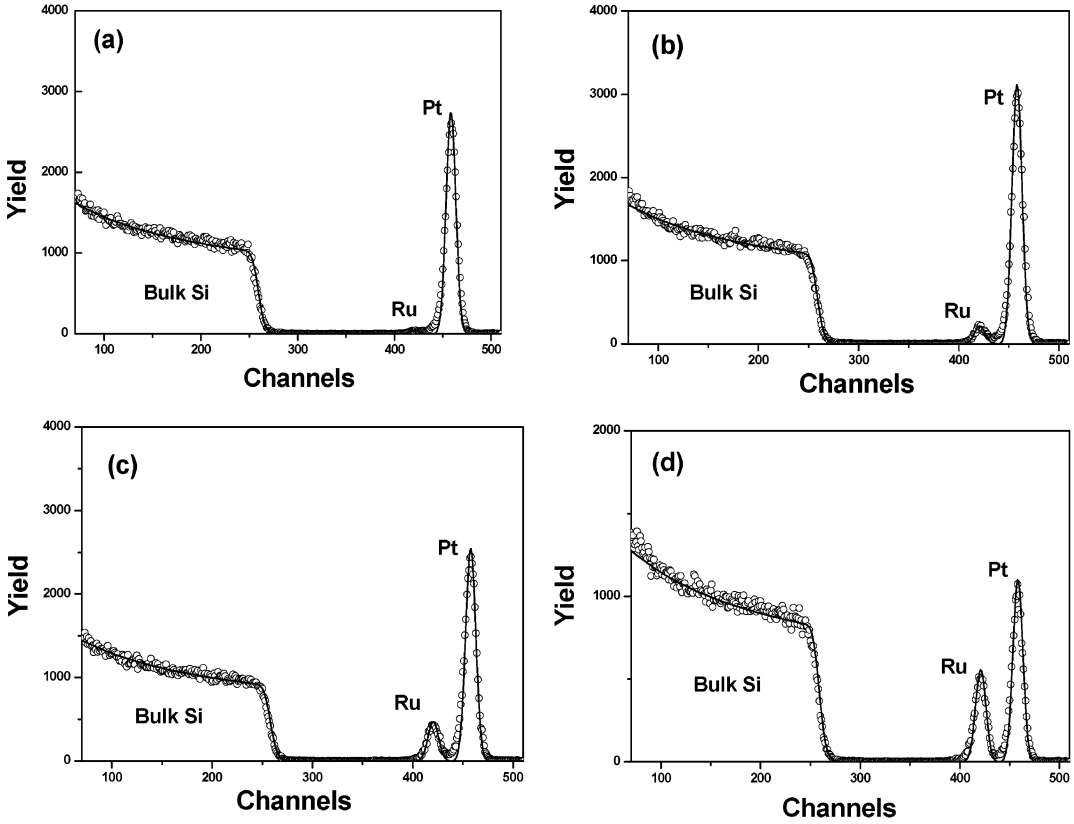

Figure 2. RBS spectra of PtRu alloy thin-film electrodes with modulated compositions of Pt and Ru: (a) PtRu-20, (b) PtRu-60, (c) PtRu-80, (d) PtRu-100.

XPS analysis, which signifies the electronic modification of Pt in the PtRu alloy catalysts. In addition, in our previous work, PtNi-based nanoparticles showed a shift in the Pt4f peak in a PtNi-based alloy structure, so-called the electronic effect.[10] On the other hand, our XPS spectra in the PtRu alloy electrodes show no evidence of electronic effects such as a shift in Pt4f, which may be due to the similar electronegativity of Pt (2.28) and Ru (2.2). Table 2 shows the chemical composition of Pt and Ru measured by Pt4f and Ru3d XPS spectra. As indicated in Table 2, it can be classified from Pt-rich chemical states (∼90 atom % Pt) of PtRu-20 to Ru-rich chemical states (∼58 atom % Ru) of PtRu-100. However, the portion of Pt on the surface layer of the PtRu alloy electrodes by XPS analysis showed a higher value of 2−5 atom % Pt than those by XRD and RBS analysis. It is noteworthy that PtRu alloy thin-film electrodes show a Pt enrichment at the surface, compared to the composition of Pt:Ru obtained by XRD data. It is known that the metal having the lower heat of sublimation tends to surface segregate in binary alloys. The heats of vaporization of Pt and Ru are 509.6 and 589.9 kJ/mol, respectively.[36] Therefore, Pt would be expected to be enriched on the surface.

The PtRu alloy thin-film electrodes such as PtRu-60, PtRu-80, and PtRu-100 show different electrochemical characteristic curves in 0.5 M H_2SO_4, depending on the surface composition of Pt and Ru, as shown in Figure 4. The electrochemical characteristic curves were modified as the amount of Ru in the PtRu electrodes was increased. As the Ru component in the electrode becomes dominant, the thickness of the double layer region, at the potential range of 0.3−0.8 V, is increased due to the hydrophilic properties of Ru. Another important electrochemical property associated with increased levels of Ru is the higher shift in potential for oxygen reduction due to the slow kinetics of Ru itself for oxygen reduction. These variations in characteristic curves indicate that well-defined PtRu alloy thin-film electrodes that contain electrochemical properties of Pt-based and Ru-based surface can be designed using a sputtering system. Furthermore, considering the catalytic activity for a methanol electrooxidation current of PtRu alloy thin-film electrodes prepared using the sputtering system, it is well-known that the 40−60 atom % of Ru in the PtRu alloy catalysts is optimal for achieving excellent catalytic activity in methanol oxidation.[37] As shown in Figure 5, among the PtRu alloy thin-film electrodes, PtRu-80 shows the highest oxidation current, i.e., the best catalytic activity for methanol oxidation in DMFC. The PtRu-80 and PtRu-100, having 40−60 atom % Ru (confirmed by XRD, RBS, XPS), showed higher methanol electrooxidation current compared to other electrodes. Accordingly, based on our structural and electrochemical understanding of PtRu alloy thin-film electrodes, the PtRu−WO_3 nanocomposite electrode containing structure-controlled PtRu nanophase with 40−60 atom % Ru in a WO_3 matrix would be fabricated to achieve highly catalytic activity in methanol electrooxdation. However, Gasteiger et al.[38] reported that well-characterized PtRu alloys showed the shift in optimum composition with temperature. A study of the dependency of methanol electooxidation on the temperature is currently underway.

PtRu−WO_3 Nanocomposite Thin-Film Electrode. Figure 6a shows a TEM image of a PtRu−WO_3 nanocomposite thin-film electrode for enhanced catalytic activity fabricated by a multigun sputtering method using Pt, Ru, and WO_3 target materials. The electrode consists of PtRu alloy nanophases 4−5 nm in size and amorphous tungsten oxidative phase. It is well-known that a well-dispersed alloy catalyst in the nanocomposite structure leads to a superior catalytic reaction of the electrode in the fuel cell. Such a configuration of the nanocomposite electrode fabricated by a multigun sputtering system is similar

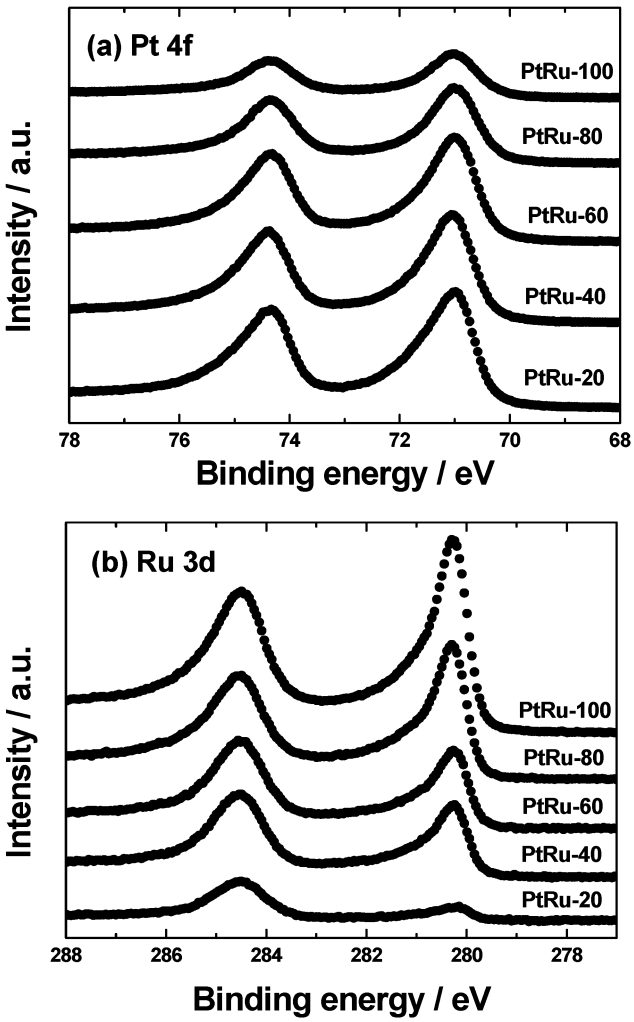

Figure 3. XPS spectra of (a) Pt4f and (b) Ru3d in PtRu alloy thin-film electrodes deposited using the sputtering system.

TABLE 2: Chemical Composition of PtRu Alloy Thin-Film Electrodes, As Determined by XPS Analysis

PtRu	Pt:Ru ratio by XPS anal.	PtRu	Pt:Ru ratio by XPS anal.
PtRu-20	90:10	PtRu-80	65:35
PtRu-40	80:20	PtRu-100	42:58
PtRu-60	75:25		

to that of conventional nanosized catalysts. The ring pattern shown in the inset of Figure 6a is consistent with the formation of nanophases in the nanocomposite electrode. In addition, although the thin-film electrode was fabricated using a sputtering system, a nanophase structure was clearly formed. In addition, as shown in Figure 6b, the crystalline plane of the nanophases can be observed in the high-resolution TEM image, suggesting an excellent crystallinity of PtRu alloy in the oxide. The (111) plane distance (*d* spacing) of the PtRu alloy nanophase in the nanocomposite electrode is reduced to 0.223 nm, compared to the (111) plane of 0.227 nm in pure Pt, indicative of good alloy formation of Pt:Ru $\sim$ 60:40 in PtRu$-$$WO_3$. The PtRu$-$$WO_3$ nanocomposite electrode, fabricated by multigun sputtering system, showed quite similar structure to PtRu-80 with the highest oxidation current, i.e. the best catalytic activity for methanol oxidation.

Figure 7a shows a plot of the specific current for methanol oxidation, methanol oxidation current per gram of catalyst, with respect to the potential of the nanocomposite electrode compared

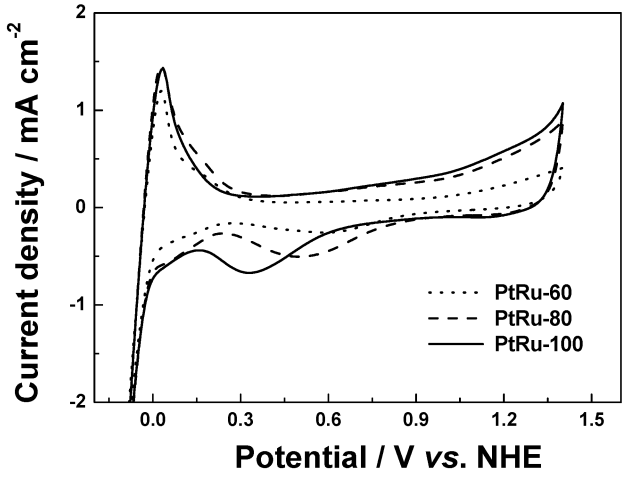

Figure 4. Cyclic voltammograms of PtRu alloy thin-film electrodes fabricated by the sputtering system in 0.5 M H_2SO_4.

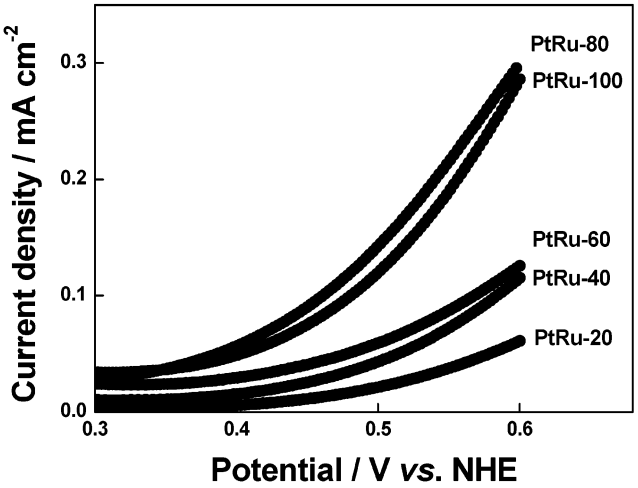

Figure 5. Methanol electrooxidation current density vs applied potential of PtRu alloy thin-film electrodes.

to a conventional PtRu nanosized catalyst (PtRu black, Johnson Matthey Co.).[30] Mass-normalized current is one of general evaluation methods to compare the catalytic activity of nanoparticles. On the other hand, the mass of catalyst in thin-film electrodes is difficult to measure. However, Witham et al. reported the mass-normalized current of sputtered PtRu alloy electrodes for methanol electrooxidation. The mass per min (μg_{PtRu} min^{-1}) of the electrode was measured. After considering growth time, the mass of the electrode can be obtained with the following equation: mass of electrode = (growth rate) $\times$ (growth time) = (5.0 μg_{PtRu} min^{-1}) $\times$ (2 min) = 10 μg_{PtRu}. The nanocomposite electrode shows excellent catalytic activity, that is, a higher methanol oxidation current compared to a conventional nanosized catalyst. The specific current of 22 A/g for the nanocomposite electrode at 0.45 V vs NHE is superior to that of 12 A/g for the case of a conventional nanosized catalyst. Another issue is the electrochemical determination of the surface area using the assumption of one hydrogen per Pt. Pt has Pt:H 1:1 stoichiometry, while pure Ru or Ru, having a solubility limit in Pt(hexagonal ruthenium phase), has been reported to have 1:2 to 3:2 Ru:H.[39,40] However, in the Pt-based fcc alloy catalysts, the hydrogen desorption charge of the alloy catalysts can be estimated by means of the assumption of 1 H adatom per surface metal atom.[41] Accordingly, assuming 210 $\mu C/cm^2$ (Pt$-$H) of polycrystalline platinum, we obtained the electrochemically active surface area of the nanocomposite

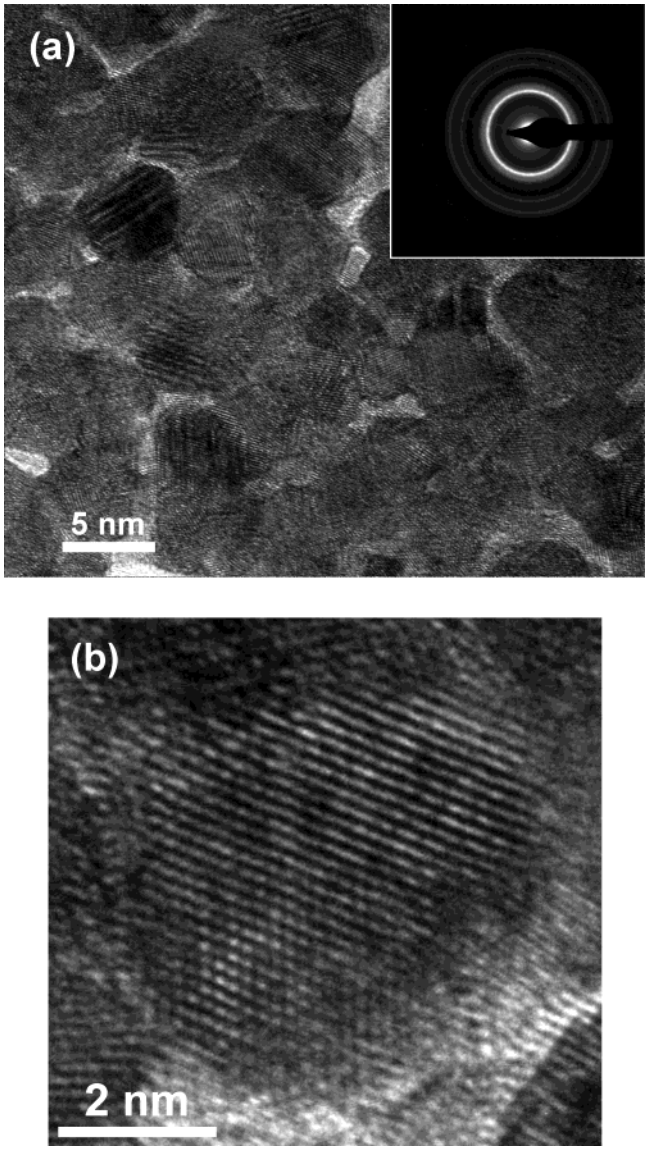

Figure 6. (a) Transmission electron micrograph (TEM) image of a PtRu−WO_3 nanocomposite thin-film electrode (The inset represents the ring pattern of the electrode by transmission electron diffraction), (b) a high-resolution TEM (HRTEM) image of alloy nanophase in the nanocomposite electrode.

electrode. On the basis of the mass and electrochemical surface area of the electrode, we obtained a specific surface area [(electrochemically active surface area) ÷ (mass of catalyst) = (5.78×10^{-4} m^2) ÷ (10×10^{-6} μg)] of 57.8 m^2/g for the nanocomposite electrode, compared to ∼40 m^2/g of PtRu alloy nanoparticle. The superior catalytic activity of a nanocomposite electrode is thought to be due to the well-dispersed catalysts in the electrodes, as evidenced by the increased active surface area. Figure 7b shows, considering the catalytic reaction produced at actual active sites, a plot of methanol oxidation current density vs applied potential.[42,43] However, although we compared and considered oxidation current per active surface area, the nanocomposite electrode (PtRu−WO_3) is superior to the conventional type electrode (PtRu unsupported catalyst) without tungsten oxide in catalytic activity for methanol oxidation. This implies that another important aspect of the enhancement in methanol oxidation in the nanocomposite electrode, the role of tungsten oxide,[44−46] is hidden, except for the increase in active surface area as the result of the homogeneous dispersion of catalysts.

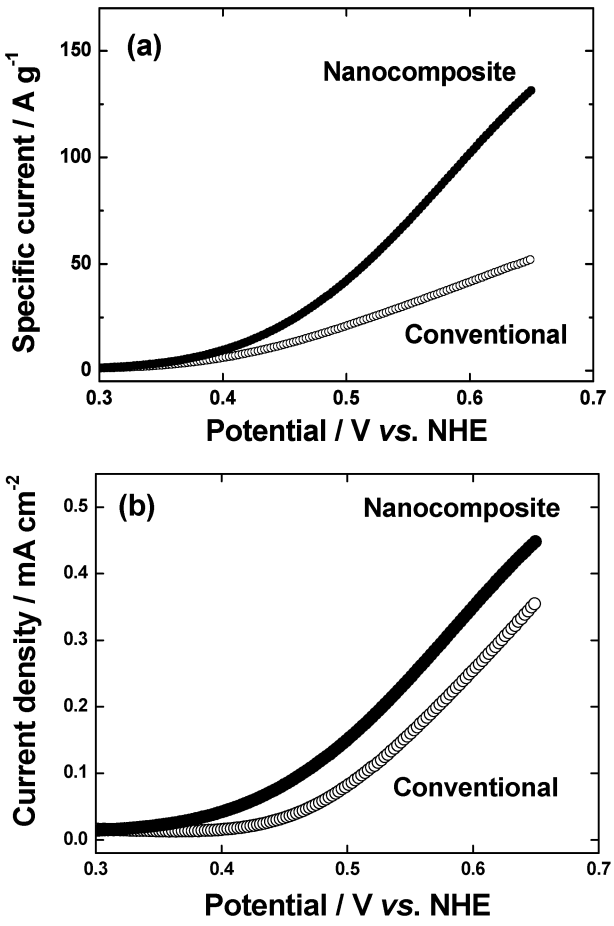

Figure 7. (a) Curve of specific current (A/g) vs potential and (b) voltammetric plot for methanol oxidation current density (mA/cm^2) vs potential of a PtRu−WO_3 nanocomposite thin-film electrode compared to a conventional, bulk-type PtRu nanosized catalyst in 2 M CH_3OH + 0.5 M H_2SO_4.

It is well-known that tungsten oxide has unique electrochromic characteristics, that is, a reversible change in optical properties under an applied potential.[47] Tungsten oxide is colored when a hydrogen ion is intercalated into the oxide, the so-called cathodic coloration. If hydrogen ions produced on the catalyst at the nanocomposite electrode during the oxidation of methanol were transferred on the tungsten oxide, these hydrogen ions would be intercalated into the tungsten oxide. Figure 8 shows variations in the transmittance in the nanocomposite electrode with respect to an applied potential compared to a tungsten oxide thin-film electrode without PtRu nanophases.[48−50] The optical signal intensity of the tungsten oxide thin-film layer was reduced at −0.3 V vs NHE, increased at +0.5 V vs NHE, and reversibly reduced at −0.3 V vs NHE. However, the fact that the nanocomposite electrode shows an exactly reverse optical signal modulation to that of the tungsten oxide electrode is surprising. In other words, the optical signal of the nanocomposite electrode was increased at −0.3 V, decreased at +0.5 V, and reversibly increased at −0.3 V. Such an opposite optical property of the nanocomposite electrode, compared to tungsten oxide, provides clear evidence in support of a modified electrochromic phenomenon due to PtRu nanophases in the tungsten oxide. This indicates that the transfer phenomenon of hydrogen ions in the tungsten oxide is affected by the PtRu nanophase embedded in the tungsten oxide. The optical intensity of the nanocomposite electrode is reduced when a potential is applied from −0.3 V to +0.5 V. Hydrogen ions produced during methanol oxidation would be transferred to the tungsten oxide in the nanocomposite

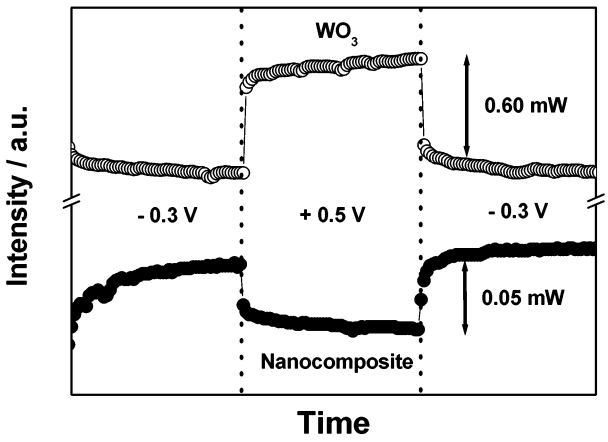

Figure 8. In situ transmittance curve of a PtRu−WO_3 nanocomposite thin-film electrode with a pulse potential of −0.3 V/+0.5 V/−0.3 V at an interval of 30 s in 2.0 M CH_3OH + 0.5 M H_2SO_4, compared to tungsten oxide as a conventional electrochromic material.

electrode at +0.5 V and would then become colored as a result of a reduced optical signal intensity, as shown in the following equation: Pt−H + WO_3 → Pt + H−WO_3. However, the pure tungsten oxide electrode without nanosized PtRu shows a bleached state at the same positive potential.

Conclusions

Alloy formation and the electrochemical properties of PtRu alloy thin-film electrodes could be modulated by appropriate control of the power of the sputtering guns. The PtRu−WO_3 nanocomposite thin-film electrode comprised of PtRu alloy nanophases with particularly selected composition and tungsten oxide showed excellent catalytic activity for methanol oxidation. The well-dispersed alloy catalyst and well-formed nanophase structure in the nanocomposite electrode would lead to a superior catalytic reaction at the electrode in a fuel cell. Furthermore, another important aspect of enhancement for methanol oxidation in the nanocomposite electrode was found to be the role of tungsten oxide, which is proven from an electrochromic phenomenon, in addition to the alloying and dispersion of the catalysts.

Acknowledgment. This work was supported by KOSEF through the Research Center for Energy Conversion and Storage and the Brain Korea 21 project from the Ministry of Education. We appreciate Korea Basic Science Institute, Busan Branch for XPS analysis.

References and Notes

(1) Klabunde, J. K. *Nanoscale Materials in Chemisty*; Wiley-Interscience: New York, 2001.
(2) Lee, S.-A.; Park, K.-W.; Choi, J.-H.; Kwon, B.-K.; Sung, Y.-E. *J. Electrochem. Soc.* **2002**, *149*, 1299.
(3) El-Sayed, M. A. *Acc. Chem. Res*. **2001**, *34*, 257.
(4) Reddington, E.; Sapienza, A.; Gurau, B.; Viswanathan, R.; Sarangapani, S.; Smotkin, E. S.; Mallouk, T. E. *Science* **1998**, *280*, 1735.
(5) Ross, P. N. In *Electrocatalysis*; Lipkowski, J.; Ross, P. N., Eds.; Wiley-VCH: New York, 1998; Ch. 2.
(6) Wieckowski, A., Ed. In *Interfacial Electrochemistry*; Marcel-Dekker: New York, 1999; Ch. 44−51.
(7) Hearth, M. P.; Hards, G. A. *Platinum Met. Rev.* **1996**, *40*, 150.
(8) Oetjen, H.-F.; Schmidt, V. M.; Stimming, U.; Trila, F. *J. Electrochem. Soc.* **1996**, *143*, 3838.
(9) Hamnett, A. *Catal. Today* **1997**, *38*, 445.
(10) Park, K.-W.; Choi, J.-H.; Kwon, B.-K.; Lee, S.-A.; Sung, Y.-E.; Ha, H.-Y.; Hong, S.-A.; Kim, H.; Wieckowski, A. *J. Phys. Chem. B.* **2002**, *106*, 1869.
(11) Gasteiger, H. A.; Markovic, N.; Ross, P. N.; Cairns, E. J. *J. Phys. Chem.* **1993**, *97*, 12020.
(12) Gasteiger, H. A.; Markovic, N.; Ross, P. N.; Cairns, E. J. *J. Electrochem. Soc.* **1994**, *141*, 1795.
(13) Gasteiger, H. A.; Markovic, N.; Ross, P. N.; Cairns, E. J. *Electrochim. Acta*. **1994**, *39*, 1825.
(14) Gasteiger, H. A.; Markovic, N.; Ross, P. N.; Cairns, E. J. *J. Phys. Chem.* **1994**, *98*, 617.
(15) Gasteiger, H. A.; Markovic, N.; Ross, P. N. *J. Phys. Chem.* **1995**, *99*, 16757.
(16) Herrero, E.; Franaszczuk, K.; Wiekowski, A. *J. Phys. Chem*. **1994**, *98*, 5074.
(17) Watanabe, M.; Motoo, S. *J. Electroanal. Chem*. **1975**, *60*, 275.
(18) Watanabe, M.; Furnnchi, Y.; Motoo, S. J. *J. Electroanal. Chem*. **1985**, *191*, 367.
(19) Watanabe, M.; Uchida, M.; Motoo, S. *J. Electroanal. Chem*. **1986**, *199*, 311.
(20) Watanabe, M.; Uchida, M.; Motoo, S. *J. Electroanal. Chem*. **1987**, *229*, 395.
(21) Wakabayashi, N.; Uchida, H.; Watanabe, M. *Electrochem. Solid-State Lett*. **2002**, *5*, 62.
(22) Ren, X.; Wilson, M. S.; Gottesfeld, S. *J. Electrochem. Soc*. **1996**, *143*, 12.
(23) Beden, B.; Lamy, C.; Tacconi, N.; Arvia, A. *Electrochim. Acta* **1990**, *35*, 691.
(24) Friedrich, K.; Geyzers, K.-P.; Linke, U.; Stimming, U. *J. Electroanal. Chem*. **1996**, *402*, 123.
(25) Ianniello, R.; Schmidt, V.; Stimming, U.; Stumper, J. *Electrochem. Acta* **1994**, *39*, 1863.
(26) Vurens, G.; Van Delft, F.; Nieuwenhuys, B. *Surf. Sci*. **1987**, *192*, 438.
(27) Parsons, R.; VanderNoot, T. *J. Electroanal. Chem*. **1988**, *257*, 9.
(28) Morse, J D.; Jankowski, F. A.; Graff, R. T.; Hayes, J. P. *J. Vac. Sci. Technol. A* **2000**, *18*, 2003.
(29) Kelley, S. C.; Deluga, G. A.; Smyrl, W. H. *Electrochem. Solid-State Lett*. **2000**, *3*, 407.
(30) Witham, C. K.; Chun, W.; Valdez, T. I.; Narayanan, S. R. *Electrochem. Solid-State Lett*. **2000**, *3*, 497.
(31) Park, K.-W.; Ahn, K.-S.; Choi, J.-H.; Nah, Y.-C.; Kim, Y.-M.; Sung, Y.-E. *Appl. Phys. Lett.* **2002**, *81*, 907.
(32) Park, K.-W.; Ahn, K.-S.; Choi, J.-H.; Nah, Y.-C.; Kim, Y.-M.; Sung, Y.-E. *Appl. Phys. Lett.* **2003**, *82*, 1090.
(33) Hutchinson, J. M. *Platinum Met. Rev*. **1989**, *16*, 88.
(34) Gasteiger, H. A.; Ross, P. N., Jr.; Cairns, E. J. *Surf. Sci*. **1993**, *293*, 67.
(35) Goodenough, J. B.; Manoharan, R.; Shukla, A. K.; Ramesh, K. V. *Chem. Mater*. **1989**, *1*, 391.
(36) Lide, D. R., Ed; In *CRC Handbook of Thermophysical and Thermochemical Data*; CRC Press: Boca Raton, FL, 1994.
(37) Liu, R.; Iddir, H.; Fan, Q.; Hou, G.; Go, A.; Ley, L. K.; Smotkin, E. S.; Sung, Y.-E.; Kim, H.; Thomas, S.; Wieckowski, A. *J. Phys. Chem. B* **2000**, *104*, 3518.
(38) Gasteiger, H. A.; Markovi, N.; Ross, P. N.; Cairns, E. J. *J. Electrochem. Soc*. **1994**, *141*, 1795.
(39) Chu, D.; Gilman. S. *J. Electrochem. Soc.* **1996**, *143*, 1685.
(40) Kinoshita, K.; Ross, P. N. *J. Electroanal. Chem*. **1977**, *78*, 313.
(41) Binder, H.; Kohling, A.; Sandstede, G. *From Electrocatalyssis to Fuel Cell*, Sandstede, G., Ed.; University of Washington Press: Seattle, WA, 1972.
(42) Schmidt, T. J.; Gasteiger, H. A.; Behm, R. J. *Electrochem. Commun*. **1999**, *1*, 1.
(43) Hamnett, A.; Weeks, S. A.; Kennedy, B. J.; Troughton, G.; Christensen, P. A. *Ber. Bunsen-Ges. Phys. Chem*. **1990**, *94*, 1014.
(44) Hobbs, B. S.; Tseung, A. C. C. *Nature* **1969**, *222*, 556.
(45) Tseung, A. C. C.; Chen, K. Y. *Catal. Today* **1997**, *38*, 439.
(46) Park, K.-W.; Ahn, K.-S.; Choi, J.-H.; Nah, Y.-C.; Sung, Y.-E. *J. Phys. Chem. B* **2003**, *107*, 4352.
(47) Granqvist, C. G. *Handbook of Inorganic Electrochromic Materials*; Elsevier Science, B. V.: Amsterdam, 1995.
(48) Ahn, K.-S.; Nah, Y.-C.; Sung, Y.-E. *J. Appl. Phys*. **2002**, *92*, 1268.
(49) Ahn, K.-S.; Nah, Y.-C.; Sung, Y.-E. *J. Appl. Phys*. **2002**, *92*, 7128.
(50) Ahn, K.-S.; Nah, Y.-C.; Cho, K.-Y.; Shin, S.-S.; Park, J.-K.; Sung, Y.-E. *Appl. Phys. Lett.* **2002**, *81*, 3930.